13th ewtec 2019 Proceedings of the 13th European Wave and Tidal Energy Conference 1-6 Sept 2019, Naples, Italy

Effects of turbines deflection over the wake dynamics and turbine performance

Clemente Gotelli, Jorge Sandoval, Wernher Brevis, and Cristián Escauriaza

Abstract—**To understand the dynamics of the turbulent wakes past marine hydrokinetic (MHK) devices, we study two configurations of turbine arrays for different deflection angles. Using a model that employs a Detached-eddy simulation (DES) flow solver, coupled with a Blade element momentum (BEM) rotor representation, we compute flows downstream of six-bladed turbines to investigate the mean velocity field, turbulence statistics, and the instantaneous dynamics of the wakes. We also perform an analysis of the wake using Proper Orthogonal Decomposition (POD) to study how the flow dynamics in the wake changes between cases. The results of the mean field characterization and modal decomposition, and in particular the spatial and temporal modifications of dominant structures are presented in terms of the energy effects associated with the selection of different geometrical layouts.**

Keywords—**3D Numerical simulations, Blade element momentum, Proper orthogonal decomposition, tidal turbines.**

I. Introduction

TIDAL currents have a significant potential to contribute to the global energy supply in the near future. High-velocity magnitudes and turbulence intensities that are developed in tidal channels are highly predictable and regular [1]. Tidal currents have the capacity of providing clean and sustainable energy through the installation of multiple hydrokinetic submerged devices.

In the last years, several experimental studies have been performed by different authors, mostly on single turbine cases, in order to further the understanding of device-flow interactions. Nevertheless, experiments with scaled turbines are limited to laboratory flows as these can cover only a short range of operating conditions and are subject to scale effects [2]. As in laboratory or in the field it is impossible to simultaneously have data for the entire spatial and temporal domain, the use of numerical modeling as a complementary tool is a good alternative as it gives complete information in both aspects.

The variety of alternatives to model turbines and its wake characteristics differs on the demand of computational resources, offering also a wide range of precision. Current modeling strategies range from simpler computationally inexpensive models that solve the flow in steady-state. Other approaches consider turbines as uniformly-loaded disks, and more complex, highly accurate and computationally expensive models like Large Eddy Simulation (LES) for solving the flow with a complete turbine geometry representation.

Gajardo et al. [3] used the DES-BEM model to simulate the experiments of Stallard et al. [4], for arrays of three-bladed turbines. In all cases, the model showed better agreement to the experimental results, compared to a RANS model employed to simulate the flows with a more detailed description of the rotor and blades. It is important to point out that these turbines have a very different geometry compared to the Sabella D10, with elongated blades and a relatively small section occupied by the hub and the nacelle.

Turbine performance and flow hydrodynamics are affected when the flow deviates from the ideal axial flow direction of design. For deflection angles between 0 and 10, a drop of 7% in the resultant peak power has been reported [5]. Also, it was shown that for the same range of deflection, the wake varies from 10 diameters (D) to 7D to get a recovery of 90% in the longitudinal velocity (u) deficit.

In this work we study the effects of turbine deflection over the device performance and the flow dynamics, in order to assess this effects and be capable of understand how they change in relation with different array configurations. We also use Proper Orthogonal Decomposition (POD) analysis to study the spatial and temporal modifications of the dominant coherent structures in terms of turbulence kinetic energy (TKE).

The paper is organized as follows: In section II we describe the numerical model based on a hybrid formulation, which captures the large-scale turbulent coherent structures of the flow with the inclusion of synthetic inflow to represent ambient turbulence. Section III contains a description of the POD technique used to analyze the wake dynamics. In Section IV we describe the study cases. In Section V we present the results of the simulations for the different configurations and analyze the results using POD. In Section VI we finally present the conclusions of this work and perspectives for future research.

THM-1744. This work was supported by Chiles Marine Energy Research & Innovation Center (MERIC) CORFO project 14CEI2-28228.

C. Gotelli is with Marine Energy Research & Innovation Center, Avenida Apoquindo 2827, 12th floor, Las Condes, Santiago, Chile. (email: clemente.gotelli@meric.cl).

J. Sandoval is with Marine Energy Research & Innovation Center, Avenida Apoquindo 2827, 12th floor, Las Condes, Santiago, Chile. (email: jorge.sandoval@meric.cl).

W. Brevis is with Hydraulics and Environmental & Mining Engineering Department, Pontificia Universidad Católica de Chile, Vicua Mackenna 4860, Santiago, Chile (email: wbrevis@ing.puc.cl).

C. Escauriaza is with Hydraulics and Environmental Engineering Department, Vicua Mackenna 4860, Santiago, Chile. Also he is with Marine Energy Research & Innovation Center, Avenida Apoquindo 2827, 12th floor, Las Condes, Santiago, Chile (email: cescauri@ing.puc.cl).

II. Numerical simulations

In order to simulate turbines and their effects over the environment, we use a Detached-Eddy Simulation (DES) model that solves flow and its turbulence coupled with a Blade Element Momentum (BEM) model. Turbines are represented by a volume V inside the mesh defined by the rotor center location O, blades radius R, and the rotor depth L, which contains the turbine blades. The turbine forces are calculated from the BEM theory and applied to all nodes located within this volume. The model resolution methodology is based on the work of [6] and was implemented on the DES flow solver by [3], for more details about the resolution algorithm the reader is referred to [3].

A. Detached-eddy simulation (DES)

The complex hydrodynamic produced by the interaction of the rotor with the flow is solved using the Unsteady Reynolds-averaged Navier-Stokes (URANS) equations for mass and momentum conservation in the DES method developed by Escauriaza & Sotiropoulos [7]–[9]. Considering the Reynolds decomposition ($U = u + u'$), URANS equations can be written in nondimensionalized form using tensor notation as:

$$\frac{\partial \tilde{u}_i}{\partial \tilde{x}_i} = 0 \tag{1}$$

$$\frac{\partial \tilde{u}_i}{\partial \tilde{t}} + \tilde{u}_j \frac{\partial \tilde{u}_i}{\partial \tilde{x}_j} = -\frac{\partial \tilde{p}}{\partial \tilde{x}_i} + \frac{1}{Re} \frac{\partial^2 \tilde{u}_j}{\partial \tilde{x}_j \partial \tilde{x}_j} - \frac{\partial}{\partial \tilde{x}_j} \langle \tilde{u}'_i \tilde{u}'_j \rangle + \tilde{S}_i \tag{2}$$

where Re is the Reynolds number ($Re = \rho U D/\mu$), $\tilde{S}_i$ is the momentum term obtained from the BEM approach, which is only considered in the nodes inside volume V. We non-dimensionalize the momentum equations, using the water depth H and the upstream free stream velocity V as length and velocity scales, respectively.

DES method uses a formulation that combines the Unsteady Reynolds-Averaged Navier-Stokes (URANS) equations with the Large Eddy Simulation (LES) model. DES was proposed and revised by Spalart et al. [10], [11]. For turbulence, it uses a one-equation eddy-viscosity model developed by Spalart & Allmaras [12].

The DES model has been used and validated by a several number of studies with different flow conditions and geometries, which validates the model ability for predicting instantaneous flow fields and turbulent structures [7]–[9], [13]–[15].

B. Blade element momentum (BEM)

The representation of the real geometry of the blade in numerical simulations needs a complex mesh that consumes significant computational resources. A less expensive alternative for representing the rotor effects over the flow is the BEM method. In this approach, the forces produced by the rotor over the flow (i.e. lift and drag) are determined instantaneously by spatially averaging the local forces acting over rings, which correspond to a radial discretization of a disk with an area equivalent to the rotor cross-section. As seen in Figure 1, for a ring of with a radius r, a constant average effect is considered, which depends only on local flow conditions and blade geometry at that specific distance from the rotor center. The advantage of this method is that the blade characteristics are considered as a source term in the momentum equations, allowing a simpler and better quality mesh to represent the interactions using less computational resources. The disadvantage is that when averaging in time, it is not possible to represent flow characteristics derived from the position of each individual blade [16].

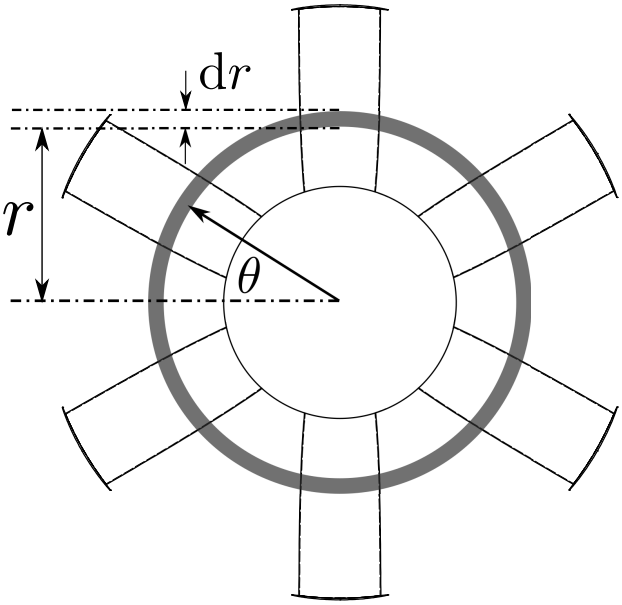

Fig. 1. Schematic view of turbine rotor. Differential radius width dr is used for rings on BEM approach. Blade characteristics depends on the distance r from the rotor center.

In our model we used the approach proposed by Creech et al. [6]. Following this approach, Lift (f_L) and Drag (f_D) forces per span unit length are calculated as:

$$f_L = \frac{1}{2} \rho c(r) U_{rel}^2 C_L(\alpha, Re) \tag{3}$$

$$f_D = \frac{1}{2} \rho c(r) U_{rel}^2 C_D(\alpha, Re) \tag{4}$$

where ρ is fluid density, U_{rel} is the relative speed between the blades and fluid, and $c(r)$ is the blade chord length at a radial distance r from the rotor center. Lift (C_L) and Drag (C_D) coefficients are functions of the blade geometry, the angle of attack α, and the local Reynolds number over the blade. The used values of C_L and C_D were given by the company owner of the turbine for different angles of attack and Reynolds numbers. The BEM method details and how the different terms were calculated can be found in [3].

C. Computational grids and boundary conditions

The boundary conditions used in this simulations are equal to those used in [17]: Non-slip condition at the bottom and walls of the flume, zero gradient at the outlet, rigid-lid at the free surface, and an unsteady inlet condition proposed by [18] that is capable of generating synthetic environmental turbulence. The

bottom of the flume has enough resolution to resolve the viscous sublayer, whereas for both lateral walls a wall function is used.

The computational domain is composed of two different zones overlapped. As it can be seen in Figure 2, the blue mesh represents the rectangular flume, whereas the red zone represents the volume V where the rotor of the turbine is located. Within this volume, the BEM forces are calculated from local instantaneous characteristics and applied into the flow. The α angle represents the deflection of the turbine relative to the ideal turbine position within the flume.

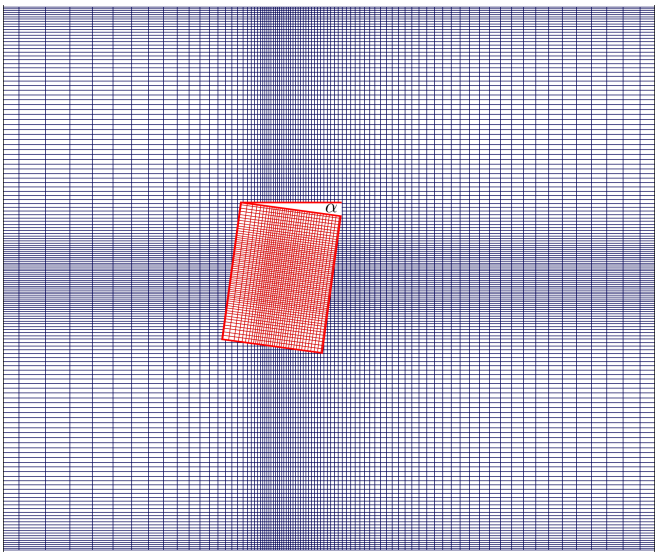

Fig. 2. Schematic representation of overlapped meshes from top view. Blue: zone #1 representing the flume, Red: zone #2 where the BEM forces are applied. The α angle is the deflection of the rotor relative to the flume domain.

III. Proper Orthogonal Decomposition

Proper Orthogonal Decomposition is a common mathematical analysis technique known by other names from other fields (e.g. Principal Component Analysis) and is closely related to singular value decomposition [19]. The POD is used to determine spatially orthogonal energy relevant structures (modes) from statistically steady-state turbulent fields, within a finite time domain, ordering them by their contribution to the total variance of the physical property being analyzed [20]. The POD analysis provides three outputs, the modes $\Phi(k)$, the eigenvalues $\lambda(k)$ of the modes, and the eigenvectors $\chi(k)$. These variables generate a complete orthogonal basis, that retains the temporal information of each mode, and together are capable of reconstruct the complete time series of the velocity field. The eigenvector can be used to identify the frequency of each mode, which provides the spatial information in the flow field [21]. The eigenvalues represent the turbulence kinetic energy of each mode, and the percentage of contribution of each mode E to the total TKE, can be obtained via:

$$E(\%) = \frac{\lambda_i}{\sum_{i=1}^{N} \lambda_i} \cdot 100 \tag{5}$$

TABLE I
Turbine and flow characteristics for all study cases

Parameter	Definition	Value	Unit
D	Rotor diameter	0.092	m
D_h	Hub diameter	0.032	m
h_h	Hub height	0.10	m
N_b	Number of blades	6	-
h	Flow height	0.30	m
Re	Reynolds number	126,667	-
Fr	Froude number	0.24	-
U_∞	Upstream velocity	0.42	$\mathrm{m{\cdot}s^{-1}}$
Ω	Rotor rotational velocity	16.6	$\mathrm{rad{\cdot}s^{-1}}$
$TSR_{1^{st}}$	Tip-speed ratio 1st case	3.65	-
$TSR_{2^{nd}}$	Tip-speed ratio 2nd case	2.01	-

The TSR showed is for the main turbine only.

IV. Study Cases

In this work, we use the cases studied experimental and numerically by [17] for the 10D turbine model of Sabella, a bidirectional hydrokinetic horizontal axis tidal turbine that was the first tidal turbine to produce electricity and be connected to the power grid [22]. In the last quarter of last year, a test turbine has been deployed for the second time at the Fromveur passage (near Brest) in France at 55 m deep [23]. The main turbine parameters and hydrodynamic conditions are presented in Table IV. The study compares two different configurations: a single turbine (ST) centered at the transverse section, and two turbines (TT) in tandem and separated by 6 turbine diameters (see Figure 3) with zero deflection or misalignment. The results showed a good agreement for the longitudinal velocity deficit measured at hub height, as can be seen in Figure 4. We also perform simulations of these configurations for different deflection angles from 0° to 10°.

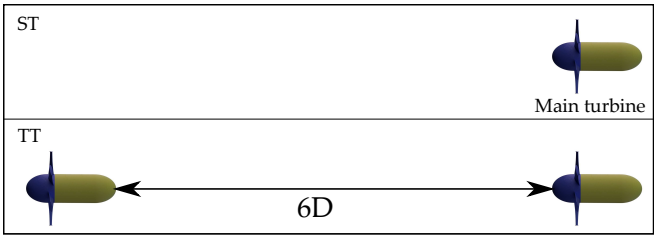

Fig. 3. Schematic view of both configurations studied. Analysis are performed in the wake of the main turbine in order to understand how the wake dynamics change when the device is deflected, and when it faces a second turbine upstream.

V. Results

Through numerical simulations we analyzed two arrays of turbines (ST and TT) under different deflection angles. The complexity of the structures generated on the wake of turbines can be visualized using the q-criterion $\left(q = \frac{1}{2}\left(\|\Omega\|^2 - \|S\|^2\right)\right)$. In Figure 5 the q-criterion iso surfaces are shown. When a turbine is located upstream of other device, the flow facing the downstream turbine is characterized by the presence

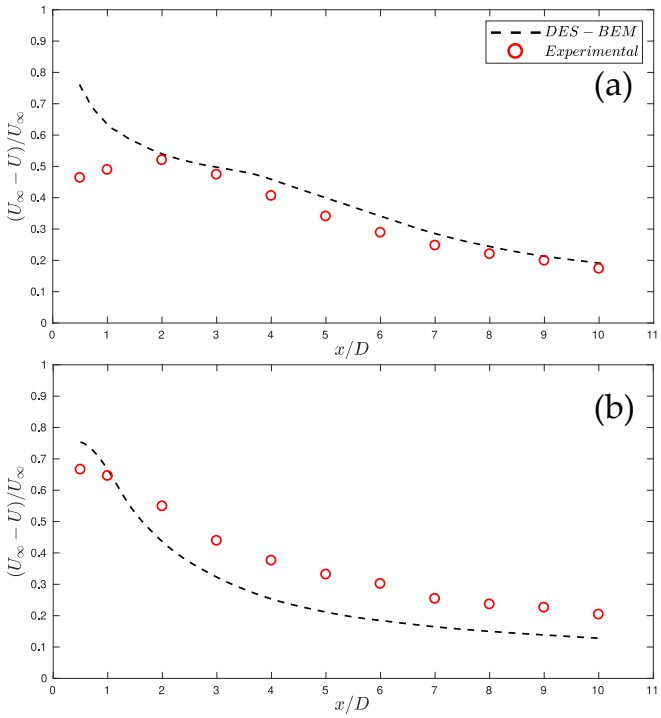

Fig. 4. Longitudinal velocity deficit comparison of DES-BEM simulations results with experimental data for (a) ST case and (b) TT case. In both cases $\alpha = 0$ and the data corresponds to the wake of the downstream turbine. The agreement between numerical simulations and experimental measurements is better for the ST case.

of complex coherent structures produced by the flow-turbine interaction. On the other hand, the momentum exchange of the wake with the surrounding flow increases and the wake gets shorter.

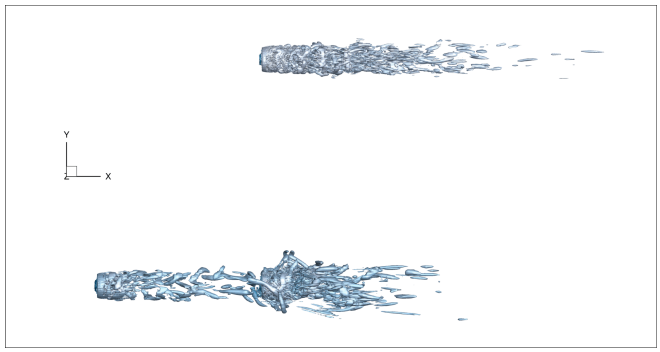

Fig. 5. Coherent structures visualization using the q criterion.

Figure 6 displays the first four modes of u in the vertical plane passing through the rotor center at a distance of 6 to 9 diameters from. Modes 1 and 2 show a great similarity, in the same way as modes 3 and 4. This result indicates that these two pairs of modes represent the same structure but displaced in space. By observing the kinetic energy associated with each mode (see Figure 6), it can be seen that both pairs of modes have similar amounts of kinetic energy, which is another indicator that are representing the same coherent structure.

The spectra of the eigenvalues are displayed in Figure 8. As expected the modes 1 and 2 have similar frequencies and peaks, and the same occurs with modes 3 and 4. These results suggest again that the

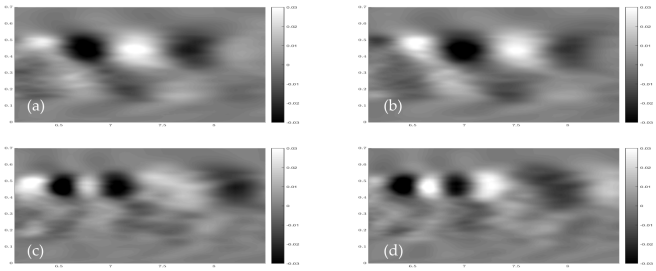

Fig. 6. First four POD modes of the vertical longitudinal plane in the far wake zone passing trough the rotor center of the turbine. (a), (b), (c) and (d) are the 1st, 2nd, 3rd and 4th modes, respectively.

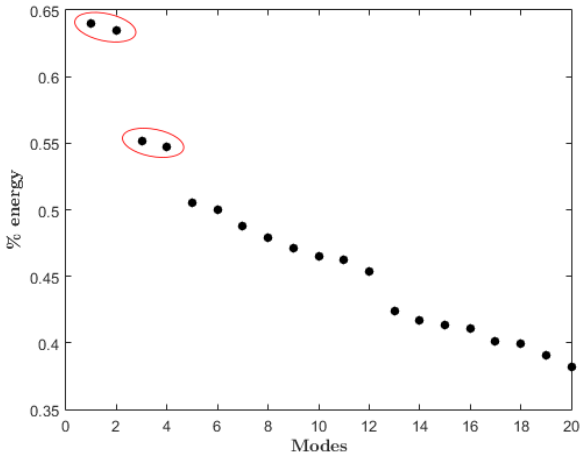

Fig. 7. Turbulence kinetic energy associated with the first twenty modes. The first four modes are separated in two pairs (mode 1 & 2, and mode 3 & 4). This indicates that both modes represents structures of similar energy.

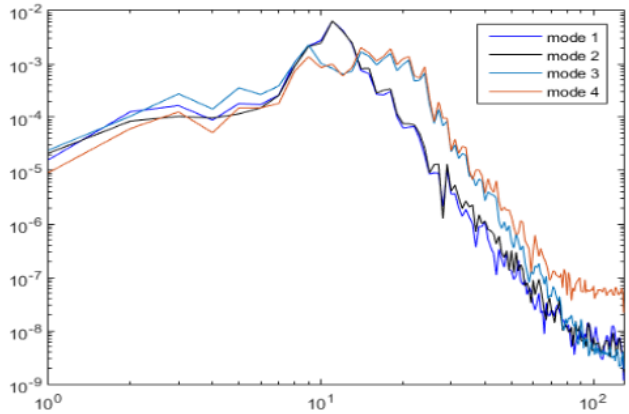

Fig. 8. POD Eigenvectors spectra for the first four modes of the plane. The coincidence of the curves indicates that the frequencies are the same within each pair.

pairs of modes mentioned before represent the same energy structure.

VI. Conclusions

A BEM model was coupled with a DES flow solver. This combined approach allowed us to capture the turbine-flow interaction in a simplified way. This model has probed previously its capacity to reproducing the mean velocity statistics of the flow when compared with laboratory experiments [17].

A POD technique was used to analyze the velocity field in different planes. The POD modes and eigenvalues obtained show two pairs of principal modes. Each pair represents an energy structure in two different times, this is corroborated by observing the eigenvectors spectra of the mentioned modes.

In future work, we will use Non-linear mode decompositions techniques to analyze the velocity fields. The complexity of the flow past turbines may require different visualization techniques which may allow us to capture interactions of coherent structures that are not being obtained by using POD.

ACKNOWLEDGEMENT

Powered@NLHPC: This research was partially supported by the supercomputing infrastructure of the NLHPC (ECM-02).

REFERENCES

[1] A. Vazquez and G. Iglesias, "Device interactions in reducing the cost of tidal stream energy," *Energy Conversion and Management*, vol. 97, pp. 428–438, 2015. [Online]. Available: http://dx.doi.org/10.1016/j.enconman.2015.03.044

[2] D. D. Apsley, T. Stallard, and P. K. Stansby, "Actuator-line CFD modelling of tidal-stream turbines in arrays," *Journal of Ocean Engineering and Marine Energy*, 2018. [Online]. Available: http://link.springer.com/10.1007/s40722-018-0120-3

[3] D. Gajardo, C. Escauriaza, and D. Ingram, "Investigation on tidal arrays with a coupled DES-BEM model," *Ocean Engineering*, submitted 2018.

[4] T. Stallard, R. Collings, T. Feng, and J. Whelan, "Interactions between tidal turbine wakes: Experimental study of a group of three-bladed rotors," *Philosophical Transactions of the Royal Society A*, vol. 371, no. 1985, pp. 1471–2962, 2013.

[5] C. H. Frost, P. S. Evans, M. J. Harrold, A. Mason-Jones, T. O'Doherty, and D. M. O'Doherty, "The impact of axial flow misalignment on a tidal turbine," *Renewable Energy*, vol. 113, pp. 1333–1344, 2017.

[6] A. Creech, W. G. Früh, and A. E. Maguire, "Simulations of an Offshore Wind Farm Using Large-Eddy Simulation and a Torque-Controlled Actuator Disc Model," *Surveys in Geophysics*, vol. 36, no. 3, pp. 427–481, 2015.

[7] C. Escauriaza and F. Sotiropoulos, *Reynolds number effects on the coherent dynamics of the turbulent horseshoe vortex system*, 2011, vol. 86, no. 2.

[8] ——, "Initial stages of erosion and bed form development in a turbulent flow around a cylindrical pier," *Journal of Geophysical Research: Earth Surface*, vol. 116, no. 3, pp. 1–24, 2011.

[9] ——, "Lagrangian model of bed-load transport in turbulent junction flows," *Journal of Fluid Mechanics*, vol. 666, pp. 36–76, jan 2011. [Online]. Available: http://www.journals.cambridge.org/abstract{_}S0022112010004192

[10] P. R. Spalart, "Comments on the feasibility of LES for wings, and on a hybrid RANS/LES approach," in *Proceedings of first AFOSR international conference on DNS/LES*. Greyden Press, 1997.

[11] ——, "Detached-Eddy Simulation," *Annual Review of Fluid Mechanics*, vol. 41, no. 1, pp. 181–202, 2009. [Online]. Available: http://www.annualreviews.org/doi/10.1146/annurev.fluid.010908.165130

[12] P. Spalart and S. Allmaras, "A one-equation turbulence model for aerodynamic flows," in *30th aerospace sciences meeting and exhibit*, 1992, p. 439.

[13] J. Paik, C. Escauriaza, and F. Sotiropoulos, "On the bimodal dynamics of the turbulent horseshoe vortex system in a wing-body junction," *Physics of Fluids*, vol. 19, no. 4, p. 045107, apr 2007. [Online]. Available: http://www.scopus.com/inward/record.url?eid=2-s2.0-78349288009{\&}partnerID=40{\&}md5=b877570b0785c3e5ee2b454bf7f30a9fhttp://aip.scitation.org/doi/10.1063/1.2716813

[14] J. Paik, F. Sotiropoulos, and F. Porté-Agel, "Detached eddy simulation of flow around two wall-mounted cubes in tandem," *International Journal of Heat and Fluid Flow*, vol. 30, no. 2, pp. 286–305, 2009. [Online]. Available: http://dx.doi.org/10.1016/j.ijheatfluidflow.2009.01.006

[15] J. Paik, . Cristian Escauriaza, F. Sotiropoulos, M. Asce, C. Escauriaza, F. Sotiropoulos, . Cristian Escauriaza, F. Sotiropoulos, and M. Asce, "Coherent structure dynamics in turbulent flows past in-stream structures: Some insights gained via numerical simulation," *Journal of Hydraulic Engineering*, vol. 136, no. 12, pp. 981–993, 2010. [Online]. Available: http://www.scopus.com/inward/record.url?eid=2-s2.0-78349288009{\&}partnerID=40{\&}md5=b877570b0785c3e5ee2b454bf7f30a9f

[16] R. Malki, I. Masters, A. J. Williams, and T. Nick Croft, "Planning tidal stream turbine array layouts using a coupled blade element momentum - computational fluid dynamics model," *Renewable Energy*, vol. 63, pp. 46–54, 2014. [Online]. Available: http://dx.doi.org/10.1016/j.renene.2013.08.039

[17] C. Gotelli, M. Musa, M. Guala, and C. Escauriaza, "Experimental and Numerical Investigation of Wake Interactions of Marine Hydrokinetic Turbines," *Energy*, submitted 2018.

[18] A. Smirnov, S. Shi, and I. Celik, "Random Flow Generation Technique for Large Eddy Simulations and Particle-Dynamics Modeling," *Journal of Fluids Engineering*, vol. 123, no. 2, p. 359, 2001.

[19] A. C. Kirby, A. Hassanzadeh, D. J. Mavriplis, and J. Naughton, "Wind Turbine Wake Dynamics Analysis Using a High-Fidelity Simulation Framework with Blade-Resolved Turbine Models," *American Institute of Aeronautics and Astronautics*, no. January, pp. 1–22, 2018.

[20] J. E. Higham, W. Brevis, C. J. Keylock, and A. Safarzadeh, "Using modal decompositions to explain the sudden expansion of the mixing layer in the wake of a groyne in a shallow flow," *Advances in Water Resources*, vol. 107, pp. 451–459, 2017. [Online]. Available: http://dx.doi.org/10.1016/j.advwatres.2017.05.010

[21] D. Lengani, D. Simoni, R. Pichler, R. Sandberg, V. Michelassi, and F. Bertini, "on the Identification and Decomposition of the Unsteady Losses in a Turbine Cascade," no. c, 2018.

[22] S. Paboeuf, P. Yen Kai Sun, L.-M. Macadré, G. Malgorn, P. Yen, K. Sun, S. Quimper, F. Laura, M. Macadré, and G. Malgorn, "Power Performance Assessment of the Tidal Turbine Sabella D10 Following IEC62600-200," in *Volume 6: Ocean Space Utilization; Ocean Renewable Energy*, vol. 6, no. Ocean Space Utilization. ASME, jun 2016, p. V006T09A007. [Online]. Available: http://proceedings.asmedigitalcollection.asme.org/pdfaccess.ashx?url=/data/conferences/asmep/89861/http://proceedings.asmedigitalcollection.asme.org/proceeding.aspx?articleid=2570928http://proceedings.asmedigitalcollection.asme.org/proceeding.aspx?doi=1

[23] Z. Zhou, M. Benbouzid, J. F. Charpentier, F. Scuiller, and T. Tang, "Developments in large marine current turbine technologies A review," pp. 852–858, 2017.